

1    **Heavy Metals and PAHs Drive Ecological and Health Risks in Chinese Water**  
2    **Level Fluctuation Zones**

3    Kang Yan <sup>a, b</sup>, Weiming Li <sup>a, b, \*</sup>, Hong Yang <sup>c, \*</sup>, Ying Xi <sup>a, b</sup>, Yixian Tan <sup>a, b</sup>, Ying  
4    Teng <sup>d</sup>, Haizhen Wang <sup>e</sup>, Julian R. Thompson<sup>f</sup>

5    <sup>a</sup> *College of Hydraulic and Environment Engineering, China Three Gorges University,  
6    Yichang, 443002, China*

7    <sup>b</sup> *Engineering Research Center of Ministry of Education of Ecological Environment in  
8    Three Gorges Reservoir Area, Yichang, 443002, China*

9    <sup>c</sup> *Department of Geography and Environmental Science, University of Reading,  
10   Whiteknights, Reading, RG6 6AB, UK*

11   <sup>d</sup> *Key Laboratory of Soil Environment and Pollution Remediation, Institute of Soil  
12   Science, Chinese Academy of Sciences, Nanjing 210008, China*

13   <sup>e</sup> *Institute of Soil and Water Resources and Environmental Science, Zhejiang Provincial  
14   Key Laboratory of Agricultural Resources and Environment, College of Environmental  
15   and Resource Sciences, Zhejiang University, Hangzhou 310058, China*

16   <sup>f</sup> *UCL Department of Geography, University College London, London WC1E 6BT, UK*

17   **Corresponding author:** Weiming Li, E-mail address: [lwm000001@126.com](mailto:lwm000001@126.com); Hong  
18   Yang, E-mail address: [h.yang4@reading.ac.uk](mailto:h.yang4@reading.ac.uk).

19      **Abstract**

20      Water-level fluctuation zones (WLFZ) adjacent to rivers, lakes and reservoirs are  
21      ecologically sensitive areas, regulating water quality and maintaining ecological health.  
22      However, research on the pollution characteristics, their spatiotemporal variability and  
23      primary sources as well as the pollution-related ecological and health risks in WLFZ  
24      soils remains limited. This study developed a comprehensive dataset of soil pollutants  
25      in Chinese WLFZs, covering nearly 3,000 sampling locations across 353 sites. The  
26      findings revealed that heavy metals and polycyclic aromatic hydrocarbons (PAHs) are  
27      the key pollutants, with the Three Gorges Reservoir identified as the primary focus area.  
28      Among the heavy metals, Cd exhibited relatively severe contamination, with Monte  
29      Carlo simulations indicating a 68.5% probability of moderate or higher contamination  
30      levels. The pollution levels of heavy metals decreased in the order: Cd > As > Pb > Cu >  
31      Zn > Cr > Hg > Ni. Despite limited non-carcinogenic risks, carcinogenic risks from As  
32      and Cd are concerning. Although the non-carcinogenic risks posed by heavy metals  
33      were limited, the average carcinogenic risk indices for children due to As (1.42e-05)  
34      and Cd (2.19e-06) were relatively high and warrant attention. Some Chinese WLFZs  
35      are contaminated with PAHs, with BaP identified as the dominant carcinogenic  
36      compound. Pollution in Chinese WLFZs is primarily attributed to coal combustion,  
37      industrial and agricultural activities, and navigation. Furthermore, current research on  
38      emerging pollutants in WLFZs remains limited, and risk assessments of their impacts  
39      on ecosystems are urgently needed. Our results provide the scientific basis for  
40      developing management strategies for pollution control in Chinese WLFZs.

41      **Keywords:** Water-level fluctuation zone; Soil pollution; Risk assessment; China

42      **1. Introduction**

43      Water-level Fluctuation Zones (WLFZ) are vulnerable and sensitive transitional  
44      area between fully aquatic and terrestrial ecosystems (Keller et al., 2021; Liu et al.,  
45      2024). They experience periodic submersion and exposure driven by water level  
46      fluctuations in adjacent aquatic environments and are widely distributed around rivers,  
47      lakes, reservoirs and other aquatic ecosystems (Pei et al., 2018). The WLFZ also  
48      constitutes a critical zone where organic matter and nutrients interact, migrate and  
49      transform between soils and overlying waters, exerting an important regulatory  
50      influence on material cycling and energy flow within the watershed (Bao et al., 2015;  
51      Liu et al., 2024; Liu et al., 2025). For instance, the repeated redox shifts characteristic  
52      of WLFZ soils enhance the mineralization of organic matter and the release of CO<sub>2</sub> and  
53      CH<sub>4</sub>, making this zone a major hotspot of greenhouse gas emissions in reservoir  
54      ecosystems (Keller et al., 2021; Yang et al., 2020; Zhang et al., 2021). Moreover,  
55      hydrological fluctuations involving alternating wetting and drying can influence the  
56      speciation and environmental behavior of pollutants (Zhang et al., 2019; Zhang et al.,  
57      2022). Under reducing conditions, heavy metals may experience valence changes that  
58      increase their mobility and bioavailability, whereas under oxidizing conditions they can  
59      be stabilized (Pei et al., 2018; Ye et al., 2021). In addition, organic contaminants such  
60      as polycyclic aromatic hydrocarbons (PAHs) may be adsorbed/desorbed under periodic  
61      wetting–drying cycles, influencing their distribution between soils and water (Han et  
62      al., 2021; Hu et al., 2017; Sun et al., 2020). Furthermore, these zones, depending on  
63      environmental conditions, can be regarded as both sources and sinks of pollutants  
64      (Zhang et al., 2019). During the non-flood season, pollutants transported from WLFZs  
65      to adjacent environments, particularly to lower-lying aquatic ecosystems, are  
66      predominantly derived from anthropogenic sources (Pei et al., 2018; Zhang et al., 2019).

67 These sources may include agricultural activities such as floodplain cultivation, as well  
68 as industrial discharges, municipal wastewater, and vehicular emissions (Fig. 1a).  
69 Under flood conditions, floodwaters may carry pollutants into WLFZs, where they  
70 subsequently accumulate through deposition processes (Hu et al., 2017).

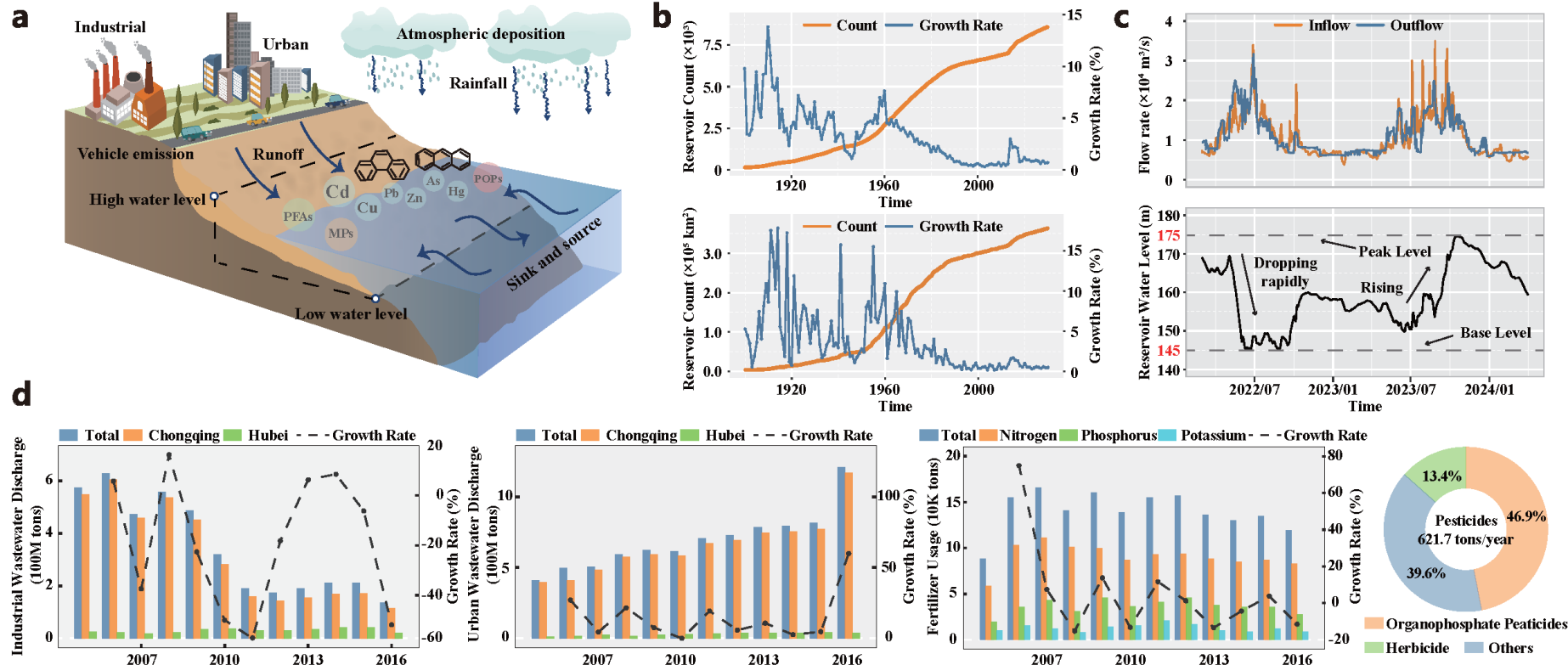
71 Human population growth and economic development have exerted substantial  
72 impacts on WLFZs, affecting both their spatial distribution and the intensity of  
73 environmental and ecological pressures they face (Keller et al., 2021; Zhang et al.,  
74 2019). For example, growing demands for renewable energy have driven a global  
75 increase in the number and size of hydropower reservoirs (Fig. 1b), consequently  
76 expanding the extent of WLFZs (Soued et al., 2022). These newly created or modified  
77 zones are frequently exposed to intensified anthropogenic disturbances, such as changes  
78 in land use, pollutant inputs, and modifications to hydrological regimes, which often  
79 collectively exacerbate ecological degradation within WLFZs (Hu et al., 2017; Pei et  
80 al., 2018). Notably, China has constructed more than 97,000 dams, including nearly 40%  
81 of the world's largest dams, with their reservoirs contributing to a substantial increase  
82 in the number and area of WLFZs (Li et al., 2018; Ye et al., 2011). For example, water  
83 levels within the Three Gorges Reservoir (TGR), the world's largest hydropower  
84 project, fluctuate between 145 and 175 meters above mean sea level in front of the dam  
85 (Fig. 1c), creating one of the largest WLFZs in the world (Bao et al., 2015; Gao et al.,  
86 2016; Yang et al., 2022). Given the substantial increases in Chinese WLFZs,  
87 establishing their soil pollution status is important for developing strategies to protect  
88 water quality and maintain ecosystem health across the nation.

89 Previous studies have shown that due to human activities, the soils in many of  
90 China's WLFZs are widely contaminated with heavy metals (Dong et al., 2023; Gao et  
91 al., 2016), polycyclic aromatic hydrocarbons (PAHs) (Han et al., 2021; Hu et al., 2017),

92 pesticides (Sun et al., 2013), and microplastics (Zhang et al., 2019). For example, in the  
93 TGR, discharges of industrial and domestic wastewater, along with agricultural runoff  
94 containing fertilizers and pesticides, are major causes of soil pollution within the  
95 reservoir's WLFZ (Fig. 1d). Notably, heavy metal contamination has been frequently  
96 reported, with cadmium (Cd), arsenic (As), and lead (Pb) being the most typical heavy  
97 metal elements that represent significant threats to human health (Ye et al., 2011; Zhang  
98 et al., 2021). For example, a study undertaken in the Wushan and Zigui sections of the  
99 TGR's WLFZ identified serious Cd pollution that was linked to high human health and  
100 ecological risks given that high-dose Cd exposure is associated with kidney and  
101 cardiovascular disease, as well as cancer (Huang et al., 2019a; Pei et al., 2018; Yan et  
102 al., 2022). Similarly, severe Cd pollution in WLFZ soil of Danjiangkou Reservoir  
103 (Hubei Province, Central China) as a result of industrial and agricultural practices has  
104 impacted water quality with implication for the safety of water supplies (Dong et al.,  
105 2023). Detection rates of persistent organic pollutants (POPs) including PAHs,  
106 pesticides, and polychlorinated biphenyls (PCBs) in the soil of Chinese WLFZs have  
107 also been relatively high (Hu et al., 2017; Wu et al., 2016; Yuan et al., 2023). Of these,  
108 PAHs have been a primary focus of research due to their carcinogenic, teratogenic, and  
109 mutagenic properties, along with their persistence in the environment (He et al., 2019;  
110 You et al., 2024). The dominant PAH species in the WLFZs include naphthalene,  
111 phenanthrene, and fluoranthene (Han et al., 2021). Although these earlier studies have  
112 assessed soil pollution within China's WLFZs, most have largely focused on specific  
113 geographical areas or individual pollutants. To the best of our knowledge, a  
114 comprehensive analysis of soil pollution across China's WLFZ is still lacking.

115 Several indices, such as the geo-accumulation index, pollution load index,  
116 Nemerow pollution index, and potential ecological risk index, have been developed for

117 assessing pollution levels and have been applied to evaluate soil pollution within  
118 WLFZs (Dong et al., 2023; Huang et al., 2023; Zhang et al., 2021). These indices can  
119 be employed to provide comprehensive assessments of soil pollution and associated  
120 ecological risks, facilitating development of effective management and remediation  
121 strategies for WLFZs (Hu et al., 2017; Pei et al., 2018). Despite the utility of these  
122 indices, current WLFZ soil pollution risk assessments rely entirely on deterministic risk  
123 assessment (DRA) methods, primarily considering the total concentration of pollutants  
124 and the most likely exposure parameters (Huang et al., 2023; Huang et al., 2024; Lin et  
125 al., 2023). These approaches lead to either underestimation or overestimation of the  
126 risks (Huang et al., 2024; Lin et al., 2023). In contrast, probabilistic risk assessment  
127 (PRA) applies stochastic methods such as Monte Carlo simulations to characterize  
128 uncertainty and variability in input parameters. This enables the estimation of a  
129 probabilistic range of potential outcomes and supports a more comprehensive  
130 understanding of risk under uncertainty (Guan et al., 2022; Wu et al., 2021).



131 **Fig. 1. Schematic diagram of the water-level fluctuation zone (WLFZ) and its potential pollution sources. a.** Environmental behavior of typical  
132 pollutants in the WLFZ. **b.** The cumulative count and area of reservoirs globally. **c.** Water level fluctuations and inflow/outflow rates in the Three  
133 Gorges Reservoir. **d.** The discharge of industrial wastewater, urban wastewater, and the application of fertilizers and pesticides in the Three Gorges  
134 Reservoir area (Source: Bulletin on the Ecological and Environmental Monitoring Results of the Three Gorges Project).  
135

136 Addressing key knowledge gaps, this study aims to: (i) systematically summarize  
137 the research on soil pollution in China's WLFZs, identifying the main pollutants of  
138 concern and the core geographical areas via a comprehensive literature review; (ii)  
139 assess soil pollution and related health risks in Chinese WLFZs via the application of a  
140 Monte Carlo analysis within the PRA framework, and propose a prioritized risk  
141 management catalogue; and (iii) identify potential pollution sources and key  
142 contaminants in China's WLFZs using the positive matrix factorization (PMF) model  
143 and quantify health risks associated with each source. The study is the first to provide  
144 a comprehensive, nationwide, understanding of soil pollution in China's WLFZs,  
145 including evaluating the associated ecological and health risks. It provides a scientific  
146 basis for developing targeted management strategies to mitigate environmental  
147 contamination and protect both human and ecosystem health.

148 **2. Materials and methods**

149 **2.1 Development of a soil pollution database for China's WLFZ**

150 A database of soil pollution in China's WLFZs was established using peer-  
151 reviewed papers retrieved from Web of Science Core Collection and the references  
152 cited by these papers (search conducted on March 18, 2024). Our search strings  
153 combined synonyms with "OR" and main elements with "AND" (Wang et al., 2024).  
154 The search terms included the following: TS (Topic Search) = (( "drawdown zone" OR  
155 "riparian zone" OR "fluctuation zone" OR "fluctuating zone" OR "water level  
156 fluctuation zone" OR "hydro-fluctuation belt" OR "littoral zone" ) AND  
157 ("contaminated" OR "polluted" OR "contamination" OR "pollution")). A Perl-based  
158 script for "front page filtering" (detailed in Fig. S1) was developed to screen the title,  
159 abstract, and keywords of each retrieved paper and to exclude irrelevant records (Fu et  
160 al., 2012; Yan et al., 2022). This study employed the Newcastle-Ottawa Scale to assess

161 the quality of each paper (Ofori et al., 2021; Yan et al., 2022), and studies lacking  
162 specific sampling location information were excluded, as the absence of such details  
163 limits effective comparison with regional soil background values. Additionally, studies  
164 focusing on deeper soil layers were also excluded, as surface soils are more  
165 representative of recent pollution inputs and have a more direct relevance to human  
166 health risk assessment (Table S1, S2) (Hu et al., 2020; Huang et al., 2019b; Yan et al.,  
167 2022). As a result, a total of 54 high-quality papers containing information about soil  
168 pollution from 353 WLFZ sites within China were identified. In total, data from  
169 individual 2,959 sampling locations were reported across these sites. Each pollutant  
170 type detected at a site was counted as a separate entry, irrespective of whether multiple  
171 pollutants were reported at the same location. Notable sites encompassed both WLFZs  
172 associated with reservoirs (e.g., the Three Gorges and Danjiangkou reservoirs) and  
173 floodplain-type zones along undammed rivers, reflecting the geographic distribution of  
174 China's major WLFZs. The following information was extracted for each paper: (i)  
175 publication information (title, keywords, publication year); (ii) sampling locations and  
176 types of pollutants; and (iii) the average values of pollutant concentration (Table S3-  
177 S4). These pollution data were obtained from tables or extracted from figures using  
178 GetData Graph Digitizer software (Eftim et al., 2017). A keyword co-occurrence  
179 network was constructed to identify the main pollutants and frequently studied regions  
180 across China (Yan et al., 2022).

## 181 **2.2 Pollution assessment of major pollutants**

### 182 **2.2.1 Index of geo-accumulation ( $I_{geo}$ )**

183 The index of geo-accumulation ( $I_{geo}$ ) can be used to estimate contamination from  
184 anthropogenic sources by eliminating the influence of background values. It has been  
185 widely applied to assess heavy metal contamination in various environments (Barbieri,

186 2016; Dong et al., 2023; Pei et al., 2018; Yan et al., 2022).  $I_{geo}$  for each heavy metal in  
187 the soil was calculated at each WLFZ sampling location using equation (1):

188

$$I_{geo} = \log_2 \frac{C_n}{1.5B_n} \quad (1)$$

189 where  $C_n$  is the concentration of heavy metal element  $n$  extracted from the selected  
190 papers (Table S3); and  $B_n$  is the geochemical background concentration of that element  
191 corresponding to the Chinese province in which each sampling site is located,  
192 determined by site's geographic coordinates (Table S5). The  $I_{geo}$  index was classified  
193 into seven categories (0-6), representing the degrees of pollution from practically  
194 uncontaminated to extremely contaminated, as detailed in Table S6.

195 **2.2.2 Risk quotient (RQ) of 16 PAHs**

196 The risk quotient (RQ) method, as described in equation (2) (Arias et al., 2023;  
197 Cao et al., 2010), was applied to evaluate the ecological risk of 16 individual PAHs in  
198 WLFZ soils across China.

199

$$RQ_{NCS} = \frac{C_{PAH}}{C_{QV}} \quad (2)$$

200 where  $C_{PAH}$  is the exposure concentration of individual PAHs, and  $C_{QV}$  is the  
201 corresponding quality value. PAH concentrations below the negligible concentrations  
202 (NCs) pose negligible risk, while those exceeding the maximum permissible  
203 concentrations (MPCs) pose unacceptable risk (Tables S7-S8). The RQ of NC and  
204 MPCs are defined using equations (3) and (4), respectively (You et al., 2024).

205

$$RQ_{NCS} = \frac{C_{PAH}}{C_{QV(NCs)}} \quad (3)$$

206

$$RQ_{MPCs} = \frac{C_{PAH}}{C_{QV(MPCs)}} \quad (4)$$

207 The total RQ is the sum of the RQ values for 16 individual PAH compounds, with  
208 only RQ values  $\geq 1$  taken into account, as shown in equations (5)-(7) (Cao et al., 2010):

209 
$$RQ_{\sum PAHs} = \sum_{i=1}^{16} RQ_i \quad (RQ \geq 1) \quad (5)$$

210 
$$RQ_{\sum PAHs (NCs)} = \sum_{i=1}^{16} RQ_{(NCs)} \quad (RQ_{(NCs)} \geq 1) \quad (6)$$

211 
$$RQ_{\sum PAHs (MPCs)} = \sum_{i=1}^{16} RQ_{(MPCs)} \quad (RQ_{(MPCs)} \geq 1) \quad (7)$$

212 Based on the computed  $RQ_{\sum PAHs}$  values, each sample site was assigned to a  
213 specific risk class, ranging from risk-free to high risk. The classification criteria for  
214 these risk levels are summarized in Table S9.

215 **2.2.3 BaP toxic equivalent concentrations (TEQ<sub>Bap</sub>)**

216 TEQ<sub>Bap</sub> was used to assess the overall contamination levels of 16 PAHs in the soil  
217 for each of the WLFZ sampling locations. This method is based on the multiplication  
218 of the concentration of each component by its corresponding toxic equivalency factor  
219 (TEF) value, followed by summing the toxic equivalency concentrations of 16 PAHs  
220 to reflect the total toxicity (Wang et al., 2011). TEQ<sub>Bap</sub> was calculated following  
221 equation (8) (Wang et al., 2011; You et al., 2024):

222 
$$TEQ_{BAP} = \sum C_{PAH} \times TEF_{PAH} \quad (8)$$

223 where  $C_{PAH}$  is the concentration of 16 PAH compounds extracted for each site from the  
224 reviewed papers, and  $TEF_{PAH}$  is the corresponding toxic equivalent factors (Table S10).

225 **2.3 Health risk assessments of major pollutants**

226 **2.3.1 Exposure assessment**

227 The main exposure pathways to contaminated soil within WLFZ sites considered  
228 in the human health risk assessment are oral ingestion, inhalation through the mouth

229 and nose, and dermal absorption (i.e. skin contact) (Hemati et al., 2024). Daily  
230 exposure doses (ADD) via ingestion (ADD<sub>Ingestion</sub>), inhalation (ADD<sub>Inhalation</sub>), and  
231 dermal uptake (ADD<sub>Dermal</sub>) were estimated using equations (9)-(11):

$$232 \quad \text{ADD}_{\text{Ingestion}} = C \times \frac{CF \times IR_{\text{Ingestion}} \times EF \times ED}{BW \times AT} \quad (9)$$

$$233 \quad \text{ADD}_{\text{Inhalation}} = C \times \frac{IR_{\text{Inhalation}} \times EF \times ED}{PEF \times BW \times AT} \quad (10)$$

$$234 \quad \text{ADD}_{\text{Dermal}} = C \times \frac{CF \times SA \times AF \times ABS \times EF \times ED}{BW \times AT} \quad (11)$$

235 where C is the concentration of specific pollutants (heavy metals and PAHs, mg/kg)  
236 obtained from the reviewed literature, and the definitions and values of the other  
237 parameters are detailed in Table S11. In addition, localized exposure parameters from  
238 the China Exposure Factors Handbook (Table S12) were incorporated into the health  
239 risk assessment for adult males and females in China, allowing for a more accurate  
240 representation of their exposure characteristics.

### 241 **2.3.2 Non-carcinogenic risk assessment**

242 Non-carcinogenic risk refers to the potential for negative effects on human health  
243 following exposure to pollutants through different pathways including ingestion,  
244 inhalation, and dermal absorption (Han et al., 2024; Hemati et al., 2024). The  
245 consequences of non-carcinogenic risks are associated with harmful health effects,  
246 including adverse reactions, physiological dysfunctions, and diseases affecting the  
247 neurological and cardiovascular systems (Gao et al., 2016; Huang et al., 2021; You et  
248 al., 2024). The hazard quotient (HQ) was used in this study to assess these non-cancer  
249 risk. It is defined as the ratio of daily exposure doses (ADD) to the reference  
250 concentration (RfC) as defined in equation (12) (Hemati et al., 2024; You et al., 2024):

$$251 \quad HQ = \sum \left( \frac{\text{ADD}_i}{\text{RfC}_i} \right) \quad (12)$$

252 where  $ADD_i$  is the daily exposure dose of pathway  $i$ , and  $RfC_i$  is the reference dose of  
253 pollutants in pathway  $i$ . The values of  $RfC_i$  are shown in Tables S13-S14. The hazard  
254 index (HI), calculated by summing the HQ of each pollutant, is used to assess the  
255 overall non-carcinogenic risk (Hemati et al., 2024). If the value of the HQ or Hazard  
256 HI exceeds 1, the population may be exposed to potential non-carcinogenic risks.

257 **2.3.3 Carcinogenic risk assessment**

258 Given the potential links of many pollutants to cancer, our study included a  
259 carcinogenic risk (CR) assessment for each of the WLFZ sampling locations. Assuming  
260 no antagonistic or synergistic interactions between pollutants, the overall carcinogenic  
261 risk can be determined as the sum of the carcinogenic risks associated with exposure to  
262 various carcinogenic pollutants through different pathways (Tepanosyan et al., 2017).

263 The CR was calculated using equation (13) (Hemati et al., 2024):

264 
$$CR = \sum (ADD_i \times SF_i) \quad (13)$$

265 where  $SF_i$  is the cancer slope factor for different pollutants via pathway  $i$ , with their  
266 values established from the literature and listed in Tables S14.

267 **2.4 Probabilistic risk modeling and sensitivity analysis**

268 The Monte Carlo method was employed for uncertainty analysis by selecting sets  
269 of model parameter values based on defined probability distributions for specific  
270 exposure factors (e.g. exposure duration, exposure frequency, ingestion rate, and  
271 inhalation rate) (Lin et al., 2023; Wu et al., 2021). This, in turn, provided probability  
272 distributions for pollutant risks for soils across the WLFZ sites. In addition, a sensitivity  
273 analysis using Monte Carlo simulation was employed to examine how a one-unit  
274 change in each individual parameter affects the model results, thereby identifying the  
275 most hazardous contaminant (Guan et al., 2022; Jafarzadeh et al., 2022). Specifically,

276 10,000 Monte Carlo simulations were performed with a 95% confidence level using the  
277 Oracle Crystal Ball plugin for Microsoft Excel (detailed in Text S1). The probability  
278 distribution settings for each parameter in the Monte Carlo simulation are summarized  
279 in Table S15. If the CR or TCR exceeds 1E-04, the population faces cancer risk, while  
280 values between 1E-04 and 1E-06 are considered within an acceptable range (Lin et al.,  
281 2023; Wu et al., 2021).

282 **2.5 Source apportionment model PMF 5.0**

283 Positive Matrix Factorization (PMF) is a source apportionment receptor model  
284 endorsed by the US Environmental Protection Agency (EPA) (Niu et al., 2020). It  
285 operates under nonnegative constraints, does not require source spectrum, and can  
286 incorporate uncertainty estimates, thereby enhancing the practicality of the analytical  
287 results (Niu et al., 2020). Within the PMF model the sample concentration data matrix  
288 ( $X$ ) is decomposed into three factor matrices as described in equation (14):

289 
$$X = GF + E \quad (14)$$

290 where  $X$  is the concentration dataset represented as a matrix with dimensions  $n \times m$ ,  $G$  is  
291 the source contribution ratio matrix ( $n \times p$ ),  $F$  is the source component spectral matrix ( $p$   
292  $\times m$ ), and  $E$  is the residuals matrix ( $n \times m$ ). Equation (14) can be transformed into equation  
293 (15) (Niu et al., 2020): And the objective function ( $Q$ ) defined by residuals and  
294 uncertainties as described in Equation (16).

295 
$$x_{ij} = \sum_{k=1}^p g_{ik} f_{kj} + e_{ij} \quad (15)$$

296 
$$Q = \sum_{i=1}^n \sum_{j=1}^m \left( \frac{e_{ij}}{u_{ij}} \right)^2 \quad (16)$$

297 where  $u_{ij}$  is uncertainty of element  $j$  in sample  $i$ , and was calculated using the lowest  
298 method detection limit (MDL), the concentration of element (heavy metals and PAHs),

299 and an error fraction ( $\sigma$ ). When  $x_{ij} \leq \text{MDL}$ ,  $u_{ij}$  was calculated using equation (17);  
300 otherwise,  $u_{ij}$  was obtained using equation (18) (Niu et al., 2020).

301

$$u_{ij} = \frac{5}{6} \times \text{MDL} \quad (17)$$

302

$$u_{ij} = \sqrt{(\sigma \times x_{ij})^2 + (0.5 \times \text{MDL})^2} \quad (18)$$

303 In this study, EPA PMF 5.0 was applied to identify potential pollution sources and  
304 quantify their contributions to soil contamination in each WLFZ sampling locations.  
305 The analysis process, following the EPA PMF 5.0 User Guide (detailed in Text S2),,  
306 used concentration data and associated uncertainty data for each pollutant as inputs,  
307 with missing values replaced by the indicator (-999) and the number of runs set to 20  
308 (Sarkar et al., 2017).

309 **2.6 Statistical data analysis and visualization**

310 The Kruskal-Wallis one-way ANOVA was applied to assess the concentration  
311 differences for the different pollutants in soils of the WLFZ sampling locations (Hemati  
312 et al., 2024). The total link strength (TLS) of keywords, calculated as the sum of a  
313 keyword's link strengths, was used to identify key research areas and major pollutants,  
314 highlighting their overall connectivity and importance (Yan et al., 2022). In addition,  
315 consistent with our previous research (Yan et al., 2023a; Yan et al., 2023b), data  
316 processing and visualization were predominantly undertaken in R using the packages  
317 “readxl” (version 1.4.3), “cowplot” (version 1.1.3), “reshape2” (version 1.4.4),  
318 “ggplot2” (version 3.5.1), and “ggspatial” (version 1.1.9).

319 **3. Results and discussion**

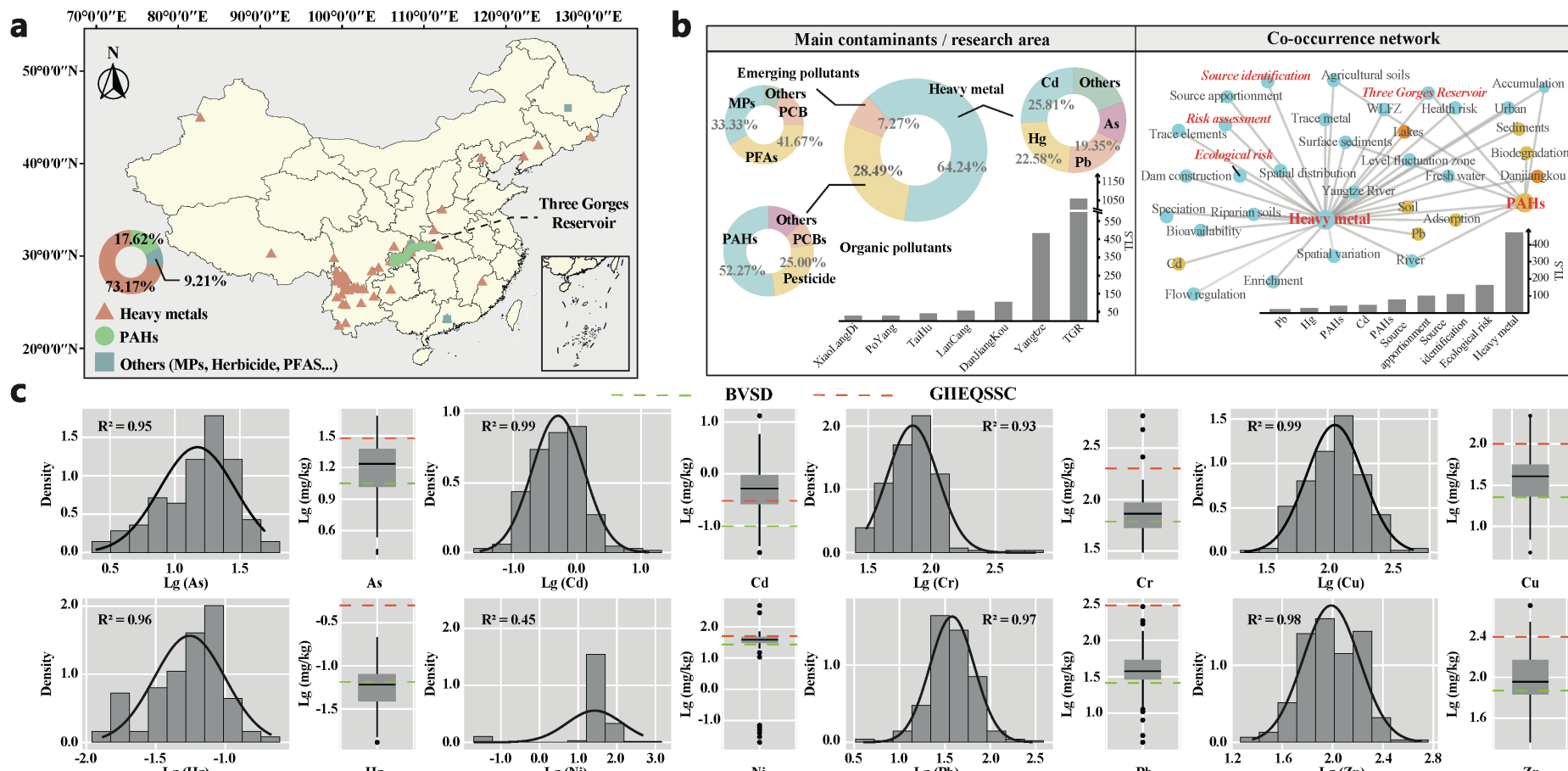
320 **3.1 Main pollutants and concentrations in soil of China's WLFZs**

321 This study ultimately obtained soil pollution data from 2,959 sampling locations  
322 across 353 sites within Chinese WLFZs. These sites are primarily located in the TGR,  
323 Danjiangkou Reservoir, the Yangtze and Lancang rivers, Taihu Lake and Poyang Lake,  
324 covering the major distribution of WLFZs in China (Fig. 2a, Tables S2-S4). Among all  
325 recorded pollutant entries across the WLFZ sites, heavy metals accounted for 73.2%,  
326 PAHs for 17.6%, and the remainder included pesticides, microplastics (MPs), and per-  
327 and polyfluoroalkyl substances (PFASs) (Fig. 2a) According to the keyword frequency  
328 statistics from the selected papers, heavy metals represented the highest proportion  
329 (total link strength (TLS) = 471), with Cd, Hg, Pb, and As being the primary focus of  
330 the research reported. Organic pollutants were primarily represented by PAHs, and the  
331 TGR emerged as the dominant location featuring within the selected papers (Fig. 2b).  
332 In the keyword network, heavy metals also occupied a central position, further  
333 highlighting their significance as a research focus for pollution in China's WLFZs.

334 The dataset revealed that the mean concentrations ( $\text{mg kg}^{-1}$ ) of the detected  
335 pollutants were as follows: As ( $18.00 \pm 10.14$ ), Cd ( $0.80 \pm 1.15$ ), Cr ( $80.04 \pm 59.16$ ),  
336 Cu ( $45.53 \pm 31.07$ ), Hg ( $0.06 \pm 0.04$ ), Ni ( $42.41 \pm 44.51$ ), Pb ( $44.47 \pm 29.53$ ), Zn  
337 ( $111.21 \pm 60.87$ ), and  $\Sigma 16$  PAHs ( $0.15 \pm 0.17$ ) (Fig. S2-S3). Compared with China's  
338 Grade II Soil Environmental Quality Standard, the exceedance rate of Cd was 69.7%  
339 (Fig. 2c), indicating that it was the most severely polluting heavy metal. With a  
340 relatively low mean concentration of  $0.80 \text{ mg kg}^{-1}$ , Cd exhibited the highest coefficient  
341 of variation (1.44) among all of the assessed pollutants, indicating pronounced relative  
342 dispersion and substantial spatial variability, potentially driven by point-source  
343 pollution or localized geochemical conditions within the WLFZ soils. Among the 16  
344 PAHs detected in WLFZ soils at varying levels, three-ring PAHs (Acpy, Acp, Flu, PA,  
345 and Ant) and four-ring PAHs (FL, Pyr, CHR, and BaA) accounted for relatively high

proportions, with mean values of 32.1% and 28.8%, respectively. In contrast, six-ring PAHs had the lowest proportion (7.5%; Fig. S3). In general, the concentrations of major pollutants such as Cd, Cr, Cu, and PAHs in WLFZ soils followed a log-normal distribution (Fig. 2, Fig. S2), with a few sampling locations within the study sites showing extremely high concentrations, likely linked to specific, spatially discrete, pollution sources (Hu et al., 2020; Yan et al., 2022). Pollutant concentrations in WLFZ soils showed no significant differences among sampling elevations (Fig. S4), as indicated by the Kruskal–Wallis test ( $P > 0.05$ ). This pattern may be attributed to varying pollutant input mechanisms across elevations (Zhang et al., 2019). Lower-elevation areas are subject to periodic flooding, which enhances pollutant accumulation through sedimentation, whereas higher elevations, although not affected by flooding, may still receive inputs from atmospheric deposition and terrestrial runoff from adjacent uplands (Ye et al., 2011). These processes together may lead to comparable overall pollutant concentrations across different elevations (Ye et al., 2011; Zhang et al., 2019). The type of WLFZs did influence pollutant concentrations across different elevations (Hu et al., 2017). Taking the TGR as an example, sampling locations were categorized into three geomorphological types based on slope characteristics (Bao et al., 2015). The first type included gently sloping areas with gradients less than 15°, typically found at lower elevations and often covered by relatively thick, uniform soil layers, where pollutants such as heavy metals and organic contaminants tend to accumulate, resulting in elevated pollutant concentrations in the soil. Slopes exhibiting a distinct inflection point, where the gradient transitions from gentle to steep, and characterized by pronounced variability in soil thickness along the slope profile constituted the second geomorphological type. Pollutant concentrations in these areas were more variable, reflecting differences in soil depth and runoff patterns. The third

371 type consisted of steep or cliff-like zones with gradients exceeding  $45^\circ$ , usually  
372 associated with thin or exposed soil layers (Bao et al., 2015). These areas are susceptible  
373 to wind and water erosion, which leads to the transport and redistribution of pollutants,  
374 with pollutants more likely to be carried to lower-slope or downstream regions rather  
375 than accumulating locally (Bao et al., 2015; Hu et al., 2017).



376

377

378

379

**Fig. 2. Primary pollutants and major research sites within existing studies. a.** Spatial distribution of primary pollutants reported in WLFZs across China. **b.** Keyword frequency and co-occurrence network for existing studies. **c.** Histograms of log-transformed data and boxplots of soil heavy metal concentrations (BVSC: Background values for soils in China. GIIEQSSC: Grade II environment quality standard for soils in China).

380 Results also indicated that concentrations of major pollutants (particularly Cd, As,  
381 Cr, and Cu) in WLFZ soil samples collected between 2010 and 2015 were significantly  
382 higher than those in samples collected before 2010 and after 2015 ( $P < 0.05$ ) (based on  
383 data from broadly comparable sites to reduce spatial variability) (Fig. S4). This trend  
384 could be attributable to China's strengthened environmental governance, including the  
385 launch of the "Water Ten Plan" in April 2015 and the "Soil Ten Plan" in May 2016.  
386 These policies were designed to reduce pollutant inputs by enforcing stricter industrial  
387 discharge regulations and improving water quality management, with several studies  
388 reporting reductions in key pollutants across various environmental media since their  
389 implementation (Huang et al., 2019b; Niu et al., 2020).

### 390 **3.2 Ecological risk of main pollutants in WLFZs**

391 Cd had the highest index of geo-accumulation ( $I_{geo}$ ), with an average value of 1.69  
392 (moderately contaminated), while Cr and Ni exhibited relatively low average  $I_{geo}$  values  
393 of -0.70 and -0.88 (practically uncontaminated), respectively (Fig. 3a). Monte Carlo  
394 simulation results showed that mean  $I_{geo}$  values reduced in the order: Cd > As > Pb >  
395 Cu > Zn > Cr > Hg > Ni, with probabilities of moderate or higher contamination levels  
396 based on cumulative frequency distribution estimated at Cd (68.5%), As (8.5%), Pb  
397 (5.2%), Cu (8.3%), Zn (3.2%), Cr (0.7%), Hg (1.4%), and Ni (8.6%).

398 The highest ecological risk level for Cd is consistent with previous findings from  
399 rivers, lakes, and sediments in China (Liu et al., 2024). The values of  $I_{geo}$  for other heavy  
400 metals were mostly classified as "practically uncontaminated" or "uncontaminated to  
401 moderately contaminated" and risk levels were lower than soils from industrial and  
402 mining areas and within acceptable thresholds (Guan et al., 2022). Low-ring PAHs  
403 exhibited higher risk quotients, with Nap (13.47) and Pyr (10.96) having the highest  
404 values that were classified as moderate-risk. In contrast, the risk quotients for CHR

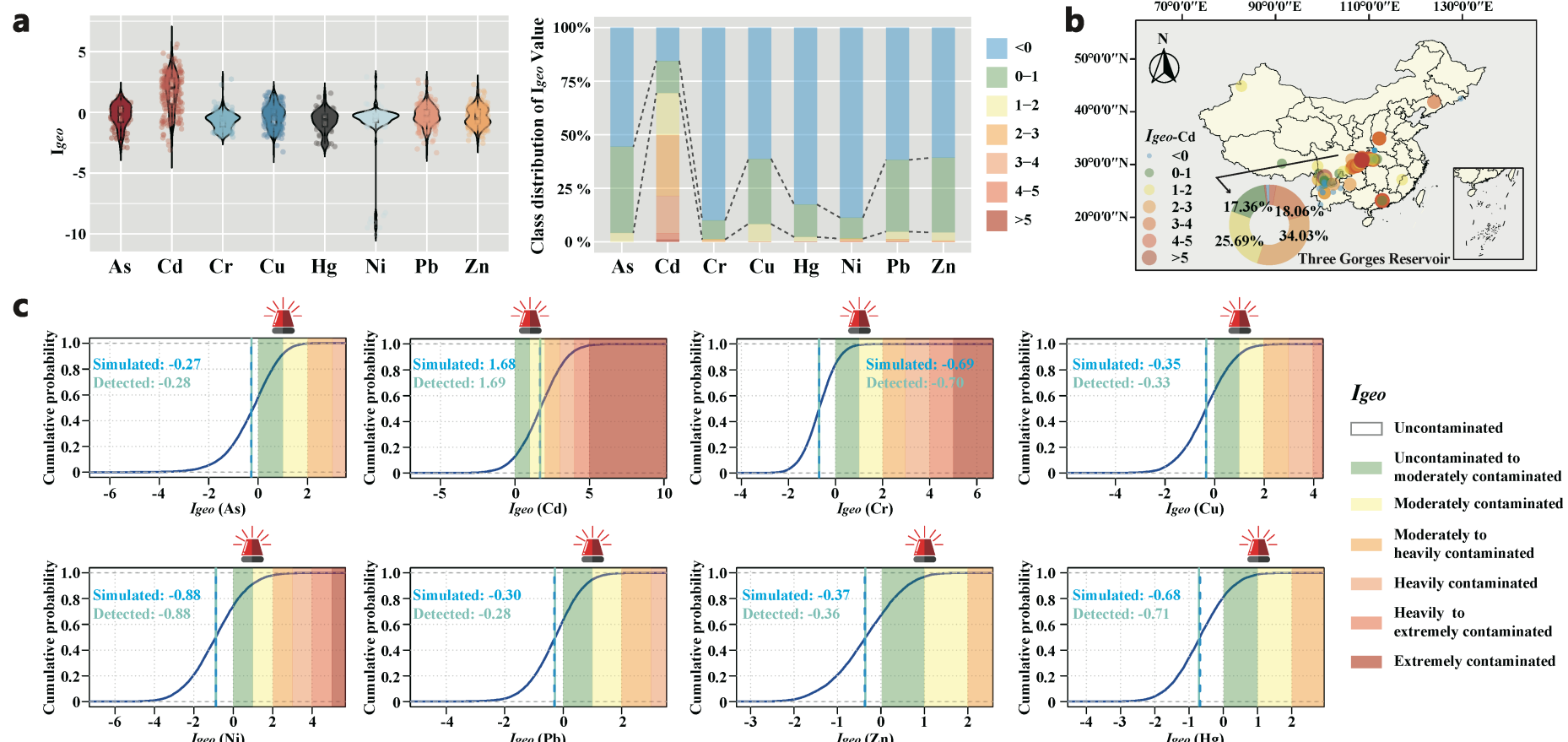
405 (0.08), DBA (0.07), and BghiP (0.07) were classified as risk-free (Fig. 4a). In most  
406 sampling locations, 2-ring and 3-ring PAHs concentrations were classed as moderate-  
407 risk, while high-ring PAHs were generally classified as risk-free (Fig. 4b). The total  
408 TEQ<sub>BaP</sub> of soil PAHs ranged from 0.09 to 67.05 ng g<sup>-1</sup>, with a mean value of 12.12 ng  
409 g<sup>-1</sup>, 52.3% of the sampling sites fell within the low to moderate risk category, with 5-  
410 ring PAHs (BbF, BaP, BkF, and DBA) contributing most to total TEQ<sub>BaP</sub> (Fig. 4c).

### 411 3.3 Health risks of main pollutants in WLFZs

412 According to the probability distributions, the hazard quotient (HQ) values for  
413 individual heavy metal elements for both adults and children were, in general, below  
414 the respective thresholds and so within safe ranges (Fig. 5a). The average HI values for  
415 adults and children were 9.66e-02 and 6.38e-01, respectively. With only 9.2% of HI  
416 values for children exceeding the critical value of 1, and none for adults. In addition,  
417 the analysis incorporating localized exposure parameters demonstrated that adult males  
418 generally exhibited higher HI values than females (Fig. S6), which is likely attributable  
419 to greater body weight and a larger dermal contact surface area. Overall, the non-  
420 carcinogenic risk caused by heavy metals in WLFZ soils was considered limited.  
421 Although the overall ecological risk was relatively low, previous research has shown  
422 that heavy metals in the soil of WLFZs can be released and redistributed through wet-  
423 dry cycles (Bao et al., 2015). As a result, these metals could potentially enter the food  
424 chain through adsorption, deposition, or diffusion. If such exposure recurs year after  
425 year, it may pose a long-term carcinogenic risk (Hu et al., 2020).

426 Carcinogenic risk values for the typical heavy metals considered in this study  
427 follow the descending order: As > Cd > Cr > Pb > Ni (Fig. 5b). Specifically, the average  
428 carcinogenic risk (CR) values for As in adults and children were 6.37e-06 and 1.42e-  
429 05, respectively, both exceeding the US EPA threshold of 1e-06 but below 1e-04,

430 indicating that the carcinogenic risk was within an acceptable level. However, reliance  
431 on average values alone may obscure localized hotspots.



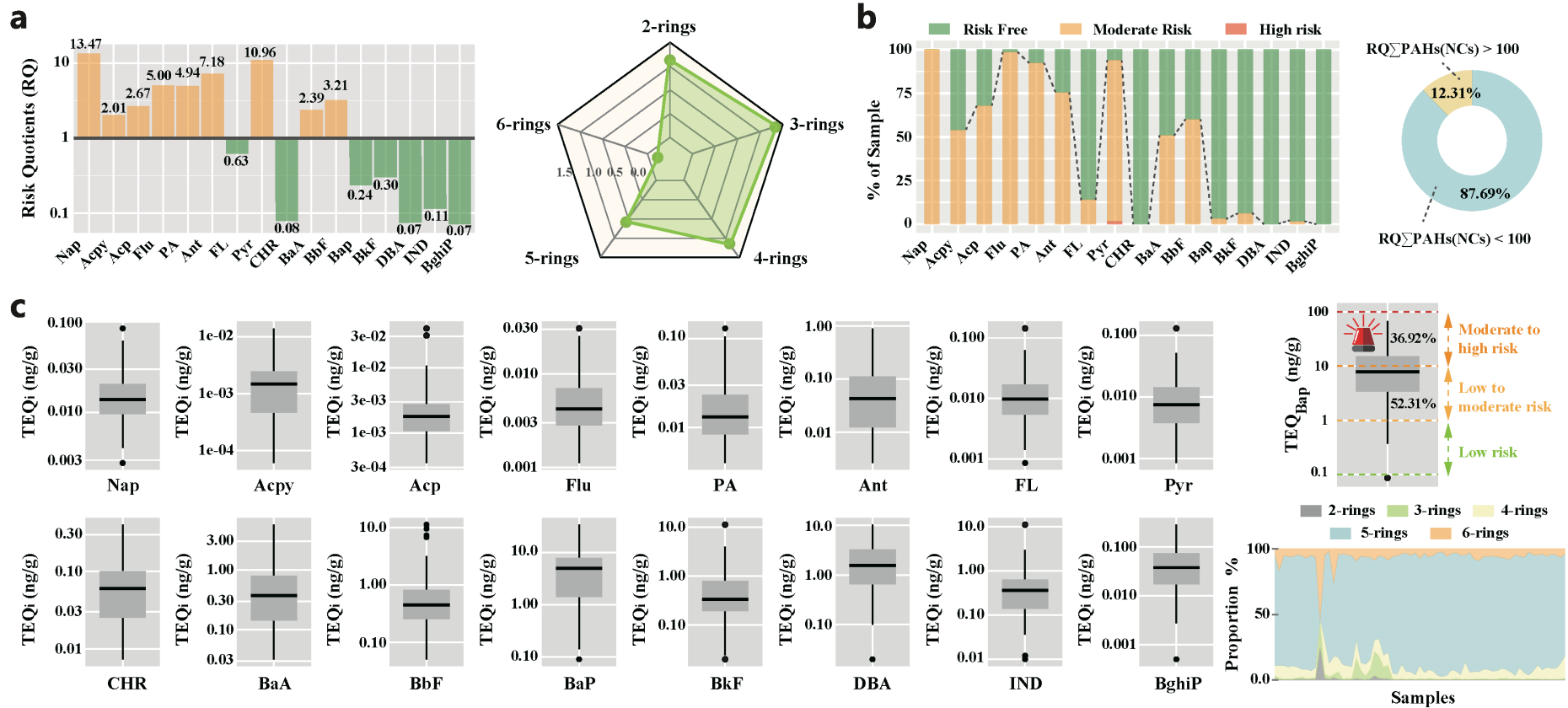
432

433

434

435

**Fig. 3. Geo-accumulation ( $I_{geo}$ ) indices of heavy metals in soil of China's WLFZs. a.** Class distribution of  $I_{geo}$  value for eight heavy metals. **b.** Geographical distribution of  $I_{geo}$  index for Cd. The donut chart represents the proportion of different  $I_{geo}$  index classes for Cd in the Three Gorges Reservoir. **c.** Cumulative probability distribution of  $I_{geo}$  indices of eight heavy metals based on Monte Carlo simulations.



436

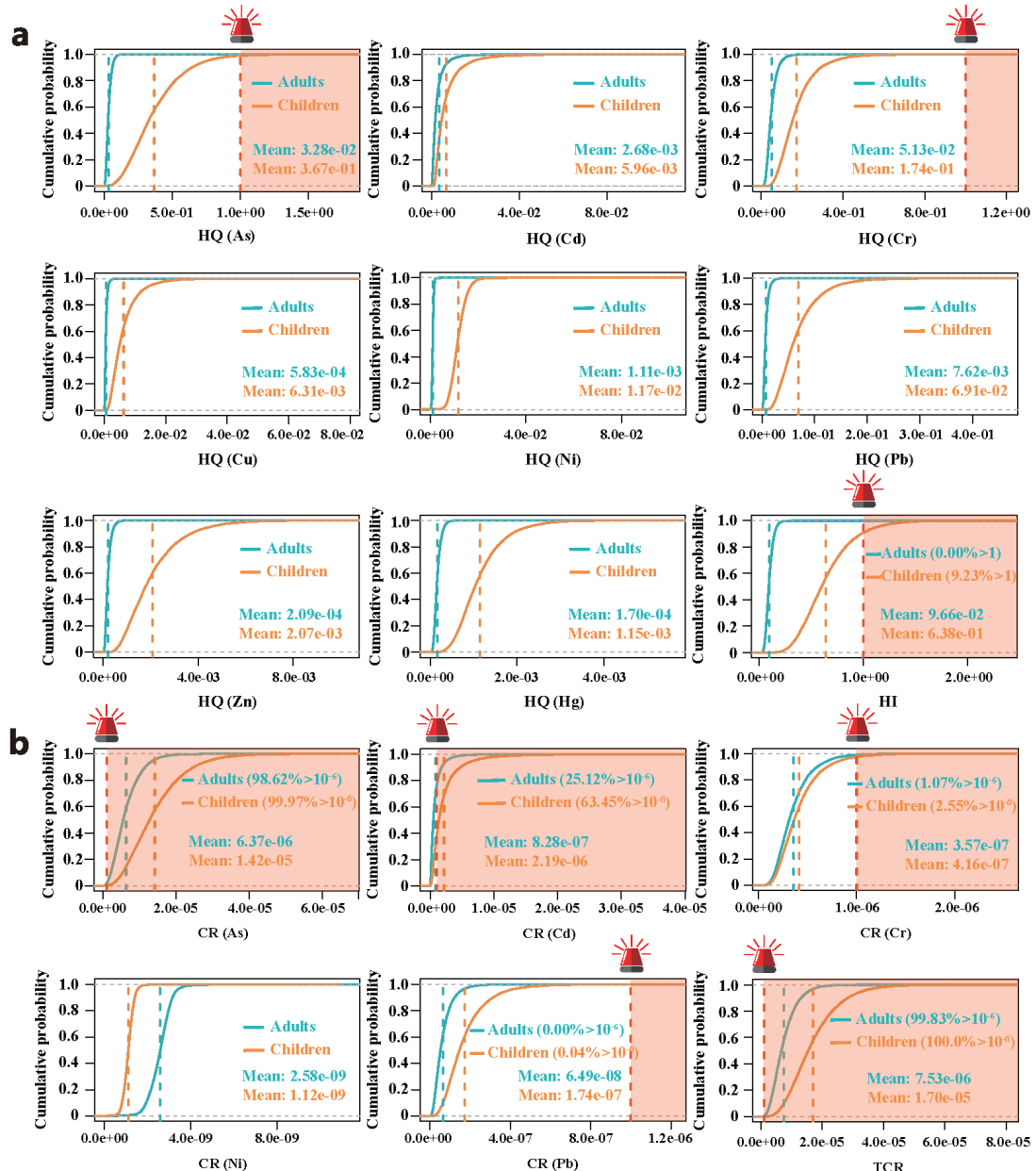
437

438

439

**Fig. 4. Ecological risks of PAHs pollution in soil of China's WLFZs. a.** Average risk quotients of 16 PAHs and radar chart indicating the log-transformed mean values of PAHs with different ring numbers. **b.** Ecological risk proportions of 16 PAHs in different samples and the ranges and proportions of total risk quotients. **c.** Toxic equivalents of PAHs and proportions of toxic equivalents for PAHs with different ring numbers.

440 Probabilistic risk analysis indicated that the probabilities of exceeding the  
441 threshold were 63.4% for children and 25.1% for adults, suggesting the presence of site-  
442 specific contamination sources that warrant further attention (Fig. 5b). Overall, As and  
443 Cd were the two heavy metals whose concentrations in WLFZ soils are currently a  
444 cause for concern. This finding is consistent with results from earlier studies on  
445 agricultural and industrial soils (Guan et al., 2022; Yan et al., 2022). The mobility and  
446 bioavailability of Cd and As make them more likely to enter the human body through  
447 the food chain, thereby increasing health risks (Huang et al., 2024; Lin et al., 2023).  
448 Previous studies suggest that As and Cd pollution in WLFZ soils may originate from  
449 fertilizer leaching from agricultural land and from industrial emissions (Ye et al., 2011;  
450 Zhang et al., 2021). Compared to adults, children are inherently more sensitive to heavy  
451 metal exposure due to their lower body weight and higher ingestion rates (e.g. frequent  
452 hand-to-mouth behaviors), which is reflected in the established risk assessment  
453 methodology used in this study (Huang et al., 2021; You et al., 2024). Although the  
454 overall concentrations of heavy metals in WLFZ soils were generally within acceptable  
455 limits, several sampling locations exhibited relatively high concentrations and potential  
456 health risks, particularly in the case of Cd and As. These elevated levels may reflect  
457 localized inputs from industrial activities, agricultural runoff, or historical pollution  
458 legacies, thereby emphasizing the need for site-specific monitoring and tailored  
459 remediation strategies (Hu et al., 2017). Therefore, future efforts should prioritize  
460 targeted assessment and management in higher-risk WLFZs or catchments with known  
461 anthropogenic pressures that are likely to elevate heavy metal pollution.

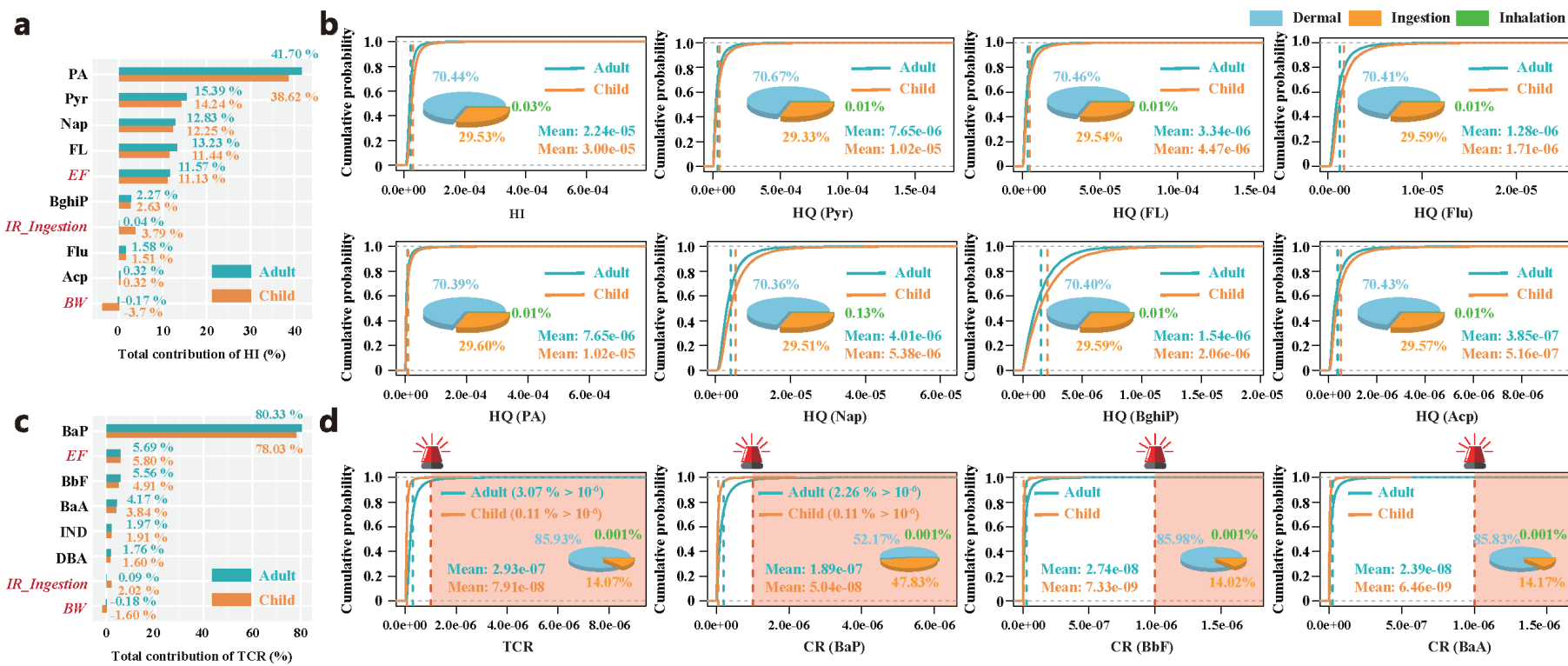


462

463 **Fig. 5. Probability distribution of hazard quotient (HQ), hazard index (HI),**  
 464 **carcinogenic risk (CR), and total carcinogenic risk (TCR) of soil heavy metals in**  
 465 **China's WLFZs. a. Probability distribution and average values of HQ for As, Cd, Cr,**  
 466 **Cu, Ni, Pb, Zn, Hg and HI for adults and children. b. Probability distribution and**  
 467 **average values of CR for As, Cd, Cr, Ni, and Pb, and TCR for adults and children.**  
 468 **Notes:** The green and orange dashed lines represent the mean values for adults and  
 469 children, respectively, while the red dashed vertical lines indicate the hazard quotient  
 470 threshold (1) and the acceptable carcinogenic risk level (1.0e-06).

471 Non-carcinogenic risks caused by PAHs were limited in WLFZ soils. The mean  
472 HI was 2.24e-05 for adults and 3.00e-05 for children, with soil concentrations of PA,  
473 Pyr, and Nap being the main influencing factors (Fig. 6). Ingestion (averaging 70.4%)  
474 was the dominant exposure pathway for non-cancer risks, followed by inhalation  
475 (averaging 29.5%), for both adults and children. This finding is consistent with previous  
476 studies suggesting that, despite PAH contamination in the soil, its impact on non-cancer  
477 risk is limited (Wu et al., 2021). However, although PAH contamination in the soil of  
478 China's WLFZs has a limited impact on non-carcinogenic health risks, the carcinogenic  
479 properties of PAHs still pose a significant health risk with long-term exposure (Han et  
480 al., 2021; Hu et al., 2017). The average total carcinogenic risk (TCR) values were 2.93e-  
481 07 for adults and 7.91e-08 for children. Based on probabilistic risk analysis using Monte  
482 Carlo simulations, the probabilities of exceeding the threshold value of 1e-06 were 3.1%  
483 for adults and 0.1% for children, respectively. Although the carcinogenic risk for adults  
484 was slightly higher than that for children, the overall risk is well below the acceptable  
485 threshold, with dermal contact and ingestion being the primary exposure pathways,  
486 while direct inhalation was negligible (Fig. 6). PAHs in WLFZ soils may enter water  
487 bodies during the period of seasonal water level rise, primarily through processes such  
488 as surface runoff, desorption into floodwaters, and physical erosion of contaminated  
489 soils (Hu et al., 2017; Yuan et al., 2023). In addition, the wet-dry cycles characteristic  
490 of WLFZs can alter soil physicochemical properties, such as total organic carbon  
491 content and particle size distribution, thereby enhancing the mobilization of PAHs (Han  
492 et al., 2021). Specifically, variations in particle size distribution can influence the soil's  
493 surface area and porosity, thereby affecting the sorption and desorption of PAHs and,  
494 consequently, their concentrations. Similarly, the health risk assessment of PAHs  
495 indicated that adult males consistently had higher TCR values than females (Fig. S7),

496 with BaP representing a carcinogenic risk of particular concern. Although overall PAH-  
497 related health risks in China's WLFZs appear to be limited, probabilistic risk  
498 assessment revealed non-negligible exceedance probabilities at specific locations,  
499 particularly for vulnerable populations such as children. Therefore, future research  
500 should focus on targeted risk-based management strategies aimed at reducing long-term  
501 human exposure in high-risk areas.



502 **Fig. 6. Probability distribution of hazard quotient (HQ), hazard index (HI), carcinogenic risk (CR), and total carcinogenic risk (TCR) of**

503 **PAHs in soil of China's WLFZs and risk sensitivity analysis of PAHs. a.** Assessment of the sensitivity of relevant parameters to the non-

504 carcinogenic risk of PAHs. **b.** Probability distribution and average values of HI and HQ. **c.** Sensitivity analysis of effective parameters in

505 carcinogenic risk of PAHs. **d.** Probability distribution of TCR and CR. The pie charts represent the proportion of carcinogenic and non-carcinogenic

506 risks associated with different exposure pathways (blue for dermal contact, orange for ingestion, and green for inhalation).

507

508      **3.4 Source apportionment of main pollutants in the WLFZs**

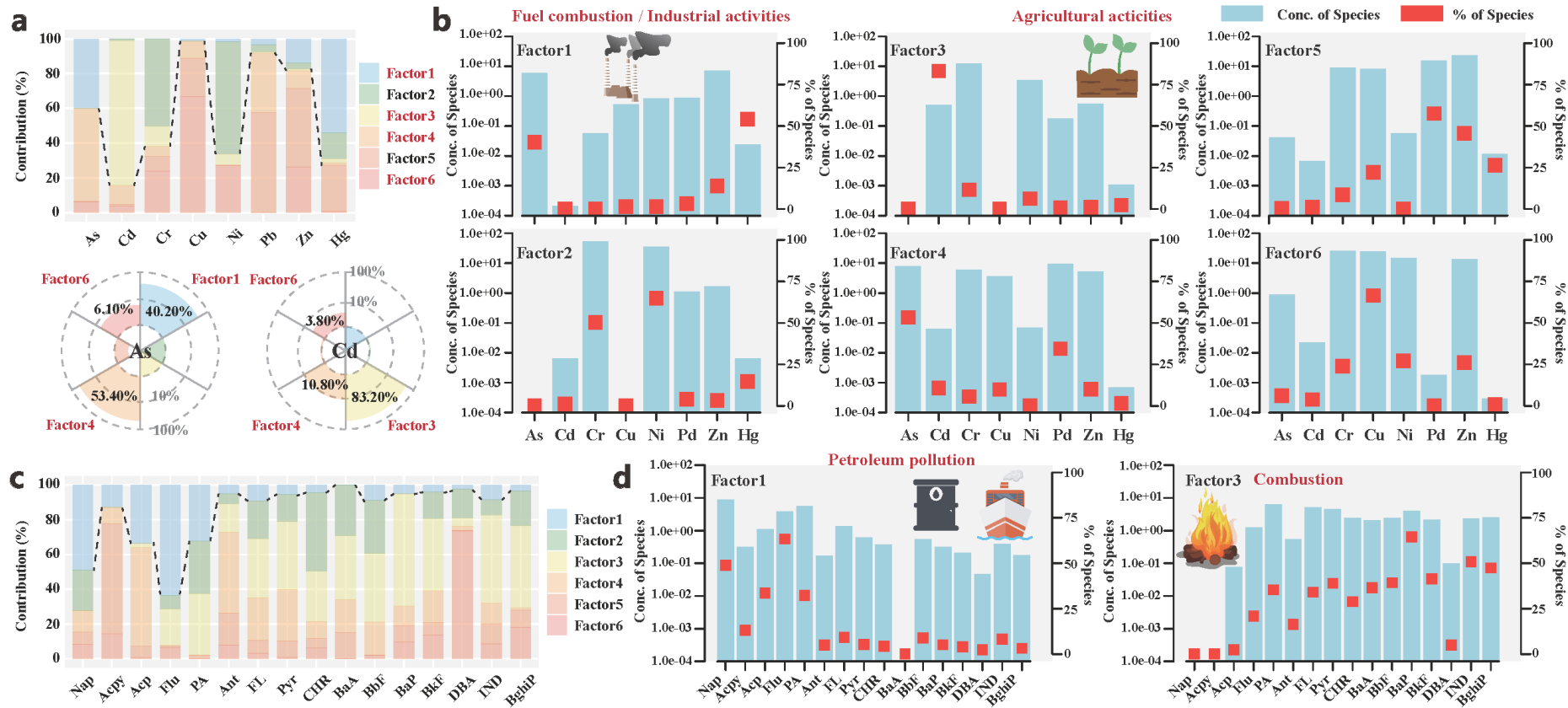
509      According to the results of the PMF model, the element As, which posed  
510      significant carcinogenic risk, was mainly associated with Factor 1 (40.2%), Factor 4  
511      (53.4%), and Factor 6 (6.1%), while the element Cd, which contributed to ecological  
512      risk, was predominantly associated with Factor 3 (83.2%) and Factor 4 (10.8%) (Fig.  
513      7). In addition, both Hg (54.2%) and Zn (14.0%) were associated with Factor 1,  
514      suggesting that this factor may be related to coal combustion and industrial activities  
515      (Cheng et al., 2023). Coal combustion has, for example, been shown to be a significant  
516      contributor to As and Hg pollution with studies demonstrating that As and trace  
517      amounts of Hg spread to surrounding soil and water bodies through smoke diffusion  
518      and particulate matter deposition (Hu et al., 2020; Liang et al., 2017; Pei et al., 2018).  
519      For example, previous research has demonstrated that widespread coal combustion in  
520      the regions surrounding the TGR contributes to the accumulation of heavy metals in the  
521      environment, with the TGR WLFZ serving as a representative area of other sites  
522      impacted by similar contamination (Liu et al., 2018). This may account for the elevated  
523      concentrations observed in several of the reviewed studies that focused on this region  
524      (Liu et al., 2018). The strong association between Cd and Factor 3 suggests that  
525      agricultural activities could be a potential source (Zhou et al., 2024). Moreover, Cd  
526      contamination in soils is widely recognized as being primarily linked to the long-term  
527      use of fertilizers and pesticides, particularly in intensively farmed regions of China as  
528      well as other countries (Dong et al., 2023). These source apportionment results are  
529      consistent with the environmental characteristics of WLFZs in China, as previous  
530      studies have also shown that WLFZs in many river basins are subjected to overlapping  
531      pressures from industrial emissions and agricultural activities, which jointly promote  
532      the pronounced accumulation and enrichment of pollutants in these areas (Hu et al.,

533 2020; Ye et al., 2011). Importantly, concentrations of heavy metals in the soils of  
534 China's WLFZs have exhibited a discernible declining trend in recent years (Fig. S4),  
535 which is plausibly attributable to the cumulative impact of successive environmental  
536 protection policies such as the “Water Ten Plan” (issued on April 2, 2015), “Soil Ten  
537 Plan” (issued on May 31, 2016), and “Environmental Protection Law of the People's  
538 Republic of China” (officially implemented from January 1, 2015), which were  
539 designed to curb emissions from coal combustion, industrial operations, and  
540 agricultural practices (Huang et al., 2024).

541 Low-ring PAHs that pose ecological risks, including Nap (48.9%), Acp (33.7%),  
542 Flu (63.4%), and PA (32.2%), were significantly associated with Factor 1, which was  
543 possibly caused by oil spills or the incomplete combustion of gasoline (Fig. 7).  
544 Specifically, Nap is a marker of petroleum pollution, and it has been suggested that in  
545 some Chinese cases PAHs in WLFZ soils may originate from oil leaks during ship  
546 navigation (Chen et al., 2013). Additionally, some chemical enterprises located in areas  
547 adjacent to WLFZs may be sources of considerable petroleum-derived pollutants, as  
548 previously reported in the TGR region (Hu et al., 2017). High-ring PAHs with  
549 significant carcinogenic risk, including BaP (64.5%), BbF (39.3%), and BkF (41.5%),  
550 were more significantly associated with Factor 3, which again may be related to  
551 combustion processes. BaP is produced during the incomplete combustion of organic  
552 matter under high-temperature conditions (Wang et al., 2023). This inference can be  
553 evidenced by isomer ratio analysis, which indicated that the combustion of grass, wood,  
554 and coal is an important source of PAHs (Fig. S5). Given the highly carcinogenic nature  
555 of PAHs, it is essential to enhance environmental regulation and pollution control not  
556 only within WLFZs but also across adjacent catchment areas, where primary pollutant  
557 sources may be located with pollutants being subsequently transported into the WLFZs.

558 Moreover, optimizing energy utilization and minimizing incomplete combustion are  
559 widely recommended as measures to mitigate high-ring PAH pollution from  
560 combustion in general that could also contribute to tackling pollution within WLFZs.

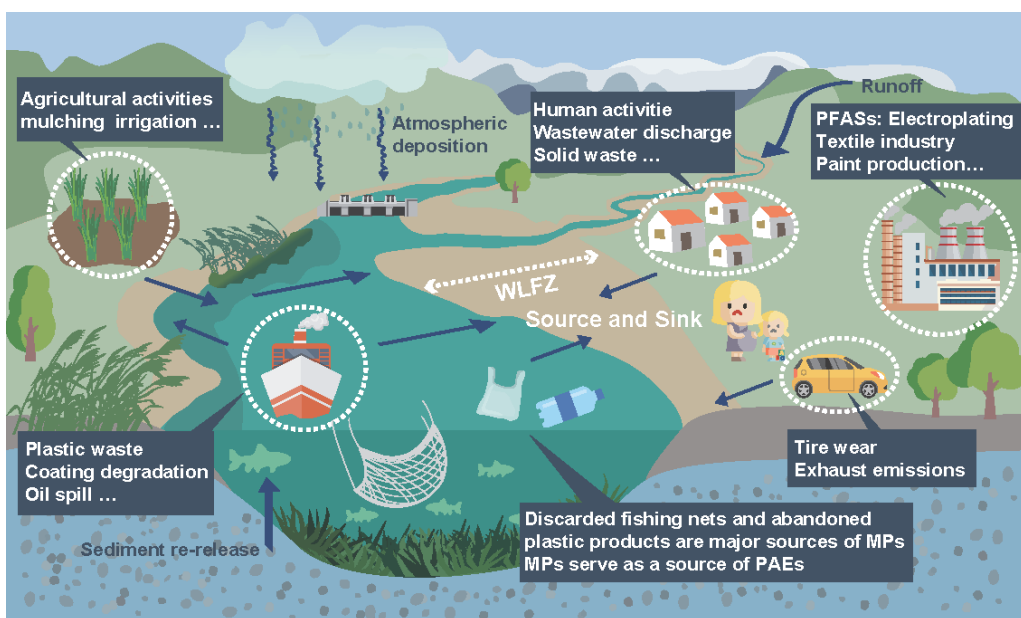
561 Furthermore, based on the source apportionment results, the management of soil  
562 pollution in Chinese WLFZs should be oriented toward region specific and source  
563 differentiated control strategies. In regions where industrial emissions and coal  
564 combustion are major contributors to soil contamination, it is essential to strengthen the  
565 monitoring of external pollutant inputs and to effectively implement emission reduction  
566 and permitting requirements for relevant industries, while areas influenced mainly by  
567 agricultural inputs should prioritize optimizing fertilizer and pesticide application and  
568 improving farmland management practices to reduce pollutant transport (Pei et al., 2018;  
569 Ye et al., 2011). The sustained implementation of these measures will play a critical  
570 role in reducing long-term pollutant loads in WLFZs and in safeguarding their  
571 ecological integrity (Bao et al., 2015).



576 **3.5 Characteristics of emerging pollutants in China's WLFZs**

577 Emerging pollutants are contaminants that have not been traditionally monitored  
578 or regulated but may pose significant risks to the environment and human health (Li et  
579 al., 2022; Zhang et al., 2019; Zhang et al., 2022). Among them, emerging pollutants of  
580 particular concern in Chinese WLFZ soils include MPs, phthalate esters (PAEs) and  
581 PFASs (Fig. 2B, Table S16). The sources of emerging pollutants in WLFZ soils are  
582 diverse and complex, likely originating from agricultural practices (e.g. mulching and  
583 fertilizer application), industrial and municipal wastewater discharges, ship operations,  
584 vehicular emissions from road traffic, and atmospheric deposition of airborne  
585 contaminants derived from combustion processes and industrial activities (Zhang et al.,  
586 2022). Although emerging pollutants share common sources and transport pathways  
587 with conventional contaminants, such as emissions from local activities and long-range  
588 transport via water and atmospheric currents, their unique environmental behaviors,  
589 persistence, and associated ecological risks in WLFZs warrant increased attention (Fig.  
590 8). The concentrations of emerging pollutants in WLFZ soils exhibit notable variations  
591 during water level fluctuations, and WLFZs can act as both sources and sinks for these  
592 pollutants (Table S16). However, research on the concentrations, environmental forms  
593 and transformation behaviors of these emerging pollutants in WLFZ soils remains  
594 limited. Existing studies also vary considerably in monitoring targets, analytical  
595 methods, spatial coverage and data completeness (Li et al., 2022; Zhang et al., 2019).  
596 This restricts robust studies on their ecological and health risks as well as source  
597 apportionment. Additionally, the lack of standardized analytical methods to measure  
598 such pollutants makes it difficult to compare results from different studies (Zhang et al.,  
599 2019). Taken together, these limitations indicate that current research on emerging  
600 pollutants in WLFZ soils remains insufficiently comprehensive and requires further

601 development. In addition, targeted and methodologically consistent investigations will  
602 be essential for establishing a robust foundation for the risk assessment and source  
603 apportionment of emerging pollutants. Moreover, source-specific mitigation measures  
604 should be implemented according to the different sources of emerging pollutants,  
605 including stricter control of agricultural non-point inputs, improved industrial and  
606 municipal wastewater treatment, and stronger regulation of atmospheric emissions to  
607 reduce external pollutant loads (Zhang et al., 2022).



609 **Fig. 8. Schematic diagram of emerging pollutant sources in WLFZ soils**

610 **3.6 Implications and limitations**

611 Although this study conducted a detailed analysis of soil pollution in China's  
612 WLFZs based on extensive published literature, employing a "front page filtering"  
613 script alongside a robust step-by-step review to ensure literature quality and minimize  
614 publication bias, certain limitations remain. The data in this study were derived from  
615 many published papers, and differences in sampling designs, extraction procedures, and  
616 analytical methods across studies (Table S2) may affect the consistency and  
617 comparability of the results. In addition, since current Chinese risk screening standards

618 and most previous studies are established on total concentrations (Table S2), this study  
619 also relied on total concentrations to estimate human health risks. However, it should  
620 be noted that total concentrations do not fully reflect the biologically effective fractions  
621 that drive toxic responses, and may overestimate the associated health risks (He et al.,  
622 2019; Yan et al., 2022). Nevertheless, we believe that this bias does not compromise  
623 the main findings of this study. This work will enhance understanding of soil pollution  
624 status and human health risks in China's WLFZ, identify priority pollutants for control,  
625 and provide critical information for the management of these fragile and ecologically  
626 sensitive areas, serving as a valuable reference for future research and policy-making.

627 Overall, this study identified multiple pollution hotspots, such as TGR, Lancang  
628 river, and Danjiangkou reservoir, along with key contaminants within China's WLFZs,  
629 offering a critical foundation for elucidating spatial pollution patterns and associated  
630 environmental risks. These findings underscore the need to prioritize high-risk areas in  
631 future monitoring and regulatory initiatives and emphasize the importance of  
632 formulating targeted, region-specific pollution mitigation strategies to protect  
633 ecosystem health and ensure public safety. In addition, it is important to note that  
634 current research on the occurrence and environmental behavior of emerging pollutants  
635 in WLFZ soils remains limited, which constrains comprehensive ecological and health  
636 risk assessments. Future investigations should strengthen efforts in this area to support  
637 the development of science-based environmental policies and management frameworks.

638 **4. Conclusions**

639 In this study, a “front page filtering” script and subsequent detailed review of  
640 published papers was employed to establish a dataset of soil pollutants in China's  
641 WLFZs that included data from 2,959 sampling locations in 353 WLFZs. The dataset  
642 included the Three Gorges Reservoir, Danjiangkou Reservoir, the Yangtze, Lancang

643 and Liao rivers, Taihu Lake and Poyang Lake with sampling sites representing the  
644 major WLFZ across China. Heavy metals were the main pollutants of concern, with Cd  
645 ( $0.80 \pm 1.15 \text{ (mg kg}^{-1}\text{)}$  being the element responsible for the most severe contamination.  
646 Simulations based on the Monte Carlo method indicated that the probability of Cd  
647 reaching moderate pollution levels was 68.5%, whereas the equivalent probabilities for  
648 As, Pb, Cu and Ni were in the range 5-10%, and those for Zn, Cr and Hg were below  
649 5%. Non-carcinogenic risks associated with heavy metals in WLFZ soils were limited.  
650 Notably, the average carcinogenic risk indices for children for As (1.42e-05) and Cd  
651 (2.19e-06) were relatively high and should be of concern. Some PAH pollution was  
652 identified in some WLFZ soils, with Nap and Pyr having the highest risk quotients,  
653 while BaP was the primary carcinogenic pollutant. The main exposure pathways were  
654 dermal contact and ingestion, while direct inhalation could be neglected. According to  
655 the results of the PMF model, coal combustion, industrial and agricultural activities,  
656 and ship navigation are the likely major sources of pollution. Although site-specific  
657 longitudinal data were unavailable, a comparative analysis of published studies from  
658 broadly similar sampling locations suggests that concentrations of major pollutants in  
659 WLFZ soils were generally lower after 2015 compared to the 2010–2015 period,  
660 potentially reflecting the effects of strengthened environmental governance measures.  
661 Future research should further explore the environmental behavior of emerging  
662 pollutants in WLFZs and conduct comprehensive risk assessments of these pollutants  
663 for both ecosystems and human health. This study contributes to the understanding of  
664 the ecological and human health risks of soil pollutants in China's WLFZs and will  
665 provide important guidance for the formulation of future environmental policies for  
666 these ecologically sensitive areas.

667 **CRediT authorship contribution statement**

668       **Kang Yan:** Writing – review & editing, Writing – original draft, Investigation,  
669       Methodology. **Weiming Li:** Writing – review & editing, Funding acquisition,  
670       Validation, Conceptualization. **Hong Yang:** Writing – review & editing, Validation,  
671       Supervision, Methodology. **Ying Xi:** Methodology, Investigation. **Yixian Tan:**  
672       Methodology. **Ying Teng:** Writing – review & editing, Supervision. **Haizhen Wang:**  
673       Methodology, Investigation. **Julian R. Thompson:** Writing – review & editing.

674       **Declaration of competing interest**

675       The authors declare that they have no known competing financial interests or  
676       personal relationships that could have appeared to influence the work reported in this  
677       paper.

678       **Data availability**

679       Supporting data are provided in Tables S2–S4 (Supporting Information).

680       **Acknowledgements**

681       This research was supported by the National Key Research and Development  
682       Programs of China (2022YFC3203905; 2022YFC3203902), Natural Science  
683       Foundation of Hubei Province (2025AFB062); National Natural Science Foundation of  
684       China (51979149), and China Three Gorges University Research Start-up Fund  
685       (2024RCKJ034).

686       **References**

687       Arias, A.H., Oliva, A.L., Ronda, A.C., Tombesi, N.B., Macchi, P., Solimano, P.,  
688       Abrameto, M., Migueles, N., 2023. Large-scale spatiotemporal variations, sources,  
689       and risk assessment of banned OCPs and PAHs in suspended particulate matter  
690       from the Negro river, Argentina. *Environ Pollut.* **320**, 121067.

691 Bao, Y., Gao, P., He, X., 2015. The water-level fluctuation zone of Three Gorges  
692 Reservoir — A unique geomorphological unit. *Earth Sci Rev.* **150**, 14-24.

693 Barbieri, M., 2016. The importance of enrichment factor (EF) and geoaccumulation  
694 index (Igeo) to evaluate the soil contamination. *J. Geol. Geophys.* **5**, 1-4.

695 Cao, Z., Liu, J., Luan, Y., Li, Y., Ma, M., Xu, J., Han, S., 2010. Distribution and  
696 ecosystem risk assessment of polycyclic aromatic hydrocarbons in the Luan River,  
697 China. *Ecotoxicology*. **19**, 827-837.

698 Chen, M., Huang, P., Chen, L., 2013. Polycyclic aromatic hydrocarbons in soils from  
699 Urumqi, China: distribution, source contributions, and potential health risks.  
700 *Environ Monit Assess.* **185**, 5639-51.

701 Cheng, B., Wang, Z., Yan, X., Yu, Y., Liu, L., Gao, Y., Zhang, H., Yang, X., 2023.  
702 Characteristics and pollution risks of Cu, Ni, Cd, Pb, Hg and As in farmland soil  
703 near coal mines. *Soil & Environmental Health.* **1**, 100035.

704 Dong, Q., Song, C., Yang, D., Zhao, Y., Yan, M., 2023. Spatial Distribution,  
705 Contamination Assessment and Origin of Soil Heavy Metals in the Danjiangkou  
706 Reservoir, China. *Int J Environ Res Public Health.* **20**, 3443.

707 Eftim, S.E., Hong, T., Soller, J., Boehm, A., Warren, I., Ichida, A., Nappier, S.P., 2017.  
708 Occurrence of norovirus in raw sewage—a systematic literature review and meta-  
709 analysis. *Water Res.* **111**, 366-374.

710 Fu, H.Z., Wang, M.H., Ho, Y.S., 2012. The most frequently cited adsorption research  
711 articles in the Science Citation Index (Expanded). *J Colloid Interface Sci.* **379**,  
712 148-156.

713 Gao, Q., Li, Y., Cheng, Q., Yu, M., Hu, B., Wang, Z., Yu, Z., 2016. Analysis and  
714 assessment of the nutrients, biochemical indexes and heavy metals in the Three  
715 Gorges Reservoir, China, from 2008 to 2013. *Water Res.* **92**, 262-274.

716 Guan, Q., Liu, Z., Shao, W., Tian, J., Luo, H., Ni, F., Shan, Y., 2022. Probabilistic risk  
717 assessment of heavy metals in urban farmland soils of a typical oasis city in  
718 northwest China. *Sci Total Environ.* **833**, 155096.

719 Han, X., Wang, F., Zhang, D., Feng, T., Zhang, L., 2021. Nitrate-assisted  
720 biodegradation of polycyclic aromatic hydrocarbons (PAHs) in the water-level-  
721 fluctuation zone of the three Gorges Reservoir, China: Insights from in situ microbial  
722 interaction analyses and a microcosmic experiment. *Environ Pollut.* **268**, 115693.

723 Han, Y., Yu, X., Cao, Y., Liu, J., Wang, Y., Liu, Z., Lyu, C., Li, Y., Jin, X., Zhang, Y.,  
724 Zhang, Y., 2024. Transport and risk of airborne pathogenic microorganisms in the  
725 process of decentralized sewage discharge and treatment. *Water Res.* **256**, 121646.

726 He, M., Yang, S., Zhao, J., Collins, C., Xu, J., Liu, X., 2019. Reduction in the exposure  
727 risk of farmer from e-waste recycling site following environmental policy  
728 adjustment: a regional scale view of PAHs in paddy fields. *Environ Int.* **133**, 105136.

729 Hemati, S., Heidari, M., Momenbeik, F., Khodabakhshi, A., Fadaei, A., Farhadkhani,  
730 M., Mohammadi-Moghadam, F., 2024. Co-occurrence of polycyclic aromatic  
731 hydrocarbons and heavy metals in various environmental matrices of a chronic  
732 petroleum polluted region in Iran; Pollution characterization, and assessment of  
733 ecological and human health risks. *J Hazard Mater.* **478**, 135504.

734 Hu, B., Shao, S., Ni, H., Fu, Z., Hu, L., Zhou, Y., Min, X., She, S., Chen, S., Huang,  
735 M., Zhou, L., Li, Y., Shi, Z., 2020. Current status, spatial features, health risks,  
736 and potential driving factors of soil heavy metal pollution in China at province  
737 level. *Environ Pollut.* **266**, 114961.

738 Hu, T., Zhang, J., Ye, C., Zhang, L., Xing, X., Zhang, Y., Wang, Y., Sun, W., Qi, S.,  
739 Zhang, Q., 2017. Status, source and health risk assessment of polycyclic aromatic

740 hydrocarbons (PAHs) in soil from the water-level-fluctuation zone of the Three  
741 Gorges Reservoir, China. *J Geochem Explor.* **172**, 20-28.

742 Huang, J., Peng, S., Mao, X., Li, F., Guo, S., Shi, L., Shi, Y., Yu, H., Zeng, G., 2019a.  
743 Source apportionment and spatial and quantitative ecological risk assessment of  
744 heavy metals in soils from a typical Chinese agricultural county. *Process Saf  
745 Environ Prot.* **126**, 339-47.

746 Huang, J., Wu, Y., Sun, J., Li, X., Geng, X., Zhao, M., Sun, T., Fan, Z., 2021. Health  
747 risk assessment of heavy metal(loid)s in park soils of the largest megacity in China  
748 by using Monte Carlo simulation coupled with Positive matrix factorization model.  
749 *J Hazard Mater.* **415**, 125629.

750 Huang, Q., Liu, M., Cao, X., Liu, Z., 2023. Occurrence of microplastics pollution in the  
751 Yangtze River: Distinct characteristics of spatial distribution and basin-wide  
752 ecological risk assessment. *Water Res.* **229**, 119431.

753 Huang, X., Li, X., Zheng, L., Zhang, Y., Sun, L., Feng, Y., Du, J., Lu, X., Wang, G.,  
754 2024. Comprehensive assessment of health and ecological risk of cadmium in  
755 agricultural soils across China: A tiered framework. *J Hazard Mater.* **465**, 133111.

756 Huang, Y., Wang, L., Wang, W., Li, T., He, Z., Yang, X., 2019b. Current status of  
757 agricultural soil pollution by heavy metals in China: A meta-analysis. *Sci Total  
758 Environ.* **651**, 3034-42.

759 Jafarzadeh, N., Heidari, K., Meshkinian, A., Kamani, H., Mohammadi, A.A., Conti,  
760 G.O., 2022. Non-carcinogenic risk assessment of exposure to heavy metals in  
761 underground water resources in Saraven, Iran: Spatial distribution, monte-carlo  
762 simulation, sensitive analysis. *Environ Res.* **204**, 112002.

763 Keller, P.S., Marcé, R., Obrador, B., Koschorreck, M., 2021. Global carbon budget of  
764 reservoirs is overturned by the quantification of drawdown areas. *Nat Geosci.* **14**,  
765 402-408.

766 Li, S., Bush, R.T., Santos, I.R., Zhang, Q., Song, K., Mao, R., Wen, Z., Lu, X.X., 2018.  
767 Large greenhouse gases emissions from China's lakes and reservoirs. *Water Res.*  
768 **147**, 13-24.

769 Li, Y., Xie, X., Zhu, Z., Liu, K., Liu, W., Wang, J., 2022. Land use driven change in  
770 soil organic carbon affects soil microbial community assembly in the riparian of  
771 Three Gorges Reservoir Region. *Appl Soil Ecol.* **176**, 104467.

772 Liang, J., Feng, C., Zeng, G., Gao, X., Zhong, M., Li, X., Li, X., He, X., Fang, Y., 2017.  
773 Spatial distribution and source identification of heavy metals in surface soils in a  
774 typical coal mine city, Lianyuan, China. *Environ Pollut.* **225**, 681-690.

775 Lin, B., Pan, P., Wei, C., Chen, X., Zhang, Z., Fan, Q., Liu, F., Liu, B., Wu, L., 2023.  
776 Health risk assessment of trace metal(loid)s in agricultural soil using an integrated  
777 model combining soil-related and plants-accumulation exposures: A case study on  
778 Hainan Island, South China. *Sci Total Environ.* **896**, 165242.

779 Liu, F., Ding, Y., Liu, J., Latif, J., Qin, J., Tian, S., Sun, S., Guan, B., Zhu, K., Jia, H.,  
780 2024. The effect of redox fluctuation on carbon mineralization in riparian soil: An  
781 analysis of the hotspot zone of reactive oxygen species production. *Water Res.* **265**,  
782 122294.

783 Liu J., Bi X., Li F., Wang P., Wu J., 2018. Source discrimination of atmospheric metal  
784 deposition by multi-metal isotopes in the Three Gorges Reservoir region, China.  
785 *Environ Pollut.* **240**, 582-589.

786 Liu, Y., Lu, Z., Wu, G., Liu, D., Xiao, H., Yang, H., Wang, H., Feng, J., 2025. Nitrogen  
787 and phosphorus release from a dominant plant in the water-level fluctuation zone of  
788 the Three Gorges Reservoir. *Aquat Sci.* **87**, 78.

789 Niu, Y., Jiang, X., Wang, K., Xia, J., Jiao, W., Niu, Y., Yu, H., 2020. Meta analysis of  
790 heavy metal pollution and sources in surface sediments of Lake Taihu, China. *Sci  
791 Total Environ.* **700**, 134509.

792 Ofori, S.A., Cobbina, S.J., Imoro, A.Z., Doke, D.A., Gaiser, T., 2021. Polycyclic  
793 aromatic hydrocarbon (PAH) pollution and its associated human health risks in the  
794 Niger Delta Region of Nigeria: a systematic review. *Environ Process.* **8**, 455-82.

795 Pei, S., Jian, Z., Guo, Q., Ma, F., Qin, A., Zhao, Y., Xin, X., Xiao, W., 2018. Temporal  
796 and spatial variation and risk assessment of soil heavy metal concentrations for  
797 water-level-fluctuating zones of the Three Gorges Reservoir. *J Soils Sediments.*  
798 **18**, 2924-34.

799 Sarkar, C., Sinha, V., Sinha, B., Panday, A.K., Rupakheti, M., Lawrence, M.G., 2017.  
800 Source apportionment of NMVOCs in the Kathmandu Valley during the SusKat-  
801 ABC international field campaign using positive matrix factorization. *Atmos Chem  
802 Phys.* **17**, 8129-56.

803 Soued, C., Harrison, J.A., Mercier-Blais, S., Prairie, Y.T., 2022. Reservoir CO<sub>2</sub> and  
804 CH<sub>4</sub> emissions and their climate impact over the period 1900–2060. *Nat Geosci.*  
805 **15**, 700-705.

806 Sun, X., Zhou, Q., Ren, W., 2013. Herbicide occurrence in riparian soils and its  
807 transporting risk in the Songhua River Basin, China. *Agron Sustain Dev.* **33**, 777-785.

808 Sun, Y., Zhang, S., Xie, Z., Lan, J., Li, T., Yuan, D., Yang, H., Xing, B., 2020.  
809 Characteristics and ecological risk assessment of polycyclic aromatic hydrocarbons

810 in soil seepage water in karst terrains, southwest China. *Ecotox Environ Saf.* **190**,  
811 110122.

812 Tepanosyan, G., Sahakyan, L., Belyaeva, O., Maghakyan, N., Saghatelian, A., 2017.  
813 Human health risk assessment and riskiest heavy metal origin identification in  
814 urban soils of Yerevan, Armenia. *Chemosphere*. **184**, 1230-40.

815 Wang, J., Wu, F., Dong, S., Wang, X., Ai, S., Liu, Z., Wang, X., 2024. Meta-analysis  
816 of the effects of microplastic on fish: Insights into growth, survival, reproduction,  
817 oxidative stress, and gut microbiota diversity. *Water Res.* **267**, 122493.

818 Wang, R., Xu, X., Yang, J., Chen, W., Zhao, J., Wang, M., Zhang, Y., Yang, Y., Huang,  
819 W., Zhang, H., 2023. BPDE exposure promotes trophoblast cell pyroptosis and  
820 induces miscarriage by up-regulating lnc-HZ14/ZBP1/NLRP3 axis. *J Hazard  
821 Mater.* **455**, 131543.

822 Wang, W., Huang, M., Kang, Y., Wang, H., Leung, A.O.W., Cheung, K.C., Wong,  
823 M.H., 2011. Polycyclic aromatic hydrocarbons (PAHs) in urban surface dust of  
824 Guangzhou, China: Status, sources and human health risk assessment. *Sci Total  
825 Environ.* **409**, 4519-27.

826 Wu, J., Bian, J., Wan, H., Sun, X., Li, Y., 2021. Probabilistic human health-risk  
827 assessment and influencing factors of aromatic hydrocarbon in groundwater near  
828 urban industrial complexes in Northeast China. *Sci Total Environ.* **800**, 149484.

829 Wu, L., Liu, L., Floehr, T., Seiler, T., Chen, L., Yuan, X., Hollert, H., 2016. Assessment  
830 of cytotoxicity and AhR-mediated toxicity of sediments from water level fluctuation  
831 zone in the Three Gorges Reservoir, China. *J Soils Sediments*. **16**, 2166-73.

832 Yan, K., Wang, H., Lan, Z., Zhou, J., Fu, H., Wu, L., Xu, J., 2022. Heavy metal  
833 pollution in the soil of contaminated sites in China: Research status and pollution  
834 assessment over the past two decades. *J Clean Prod.* **373**, 133780.

835 Yan, K., You, Q., Wang, S., Zou, Y., Chen, J., Xu, J., Wang, H., 2023a. Depth-  
836 dependent patterns of soil microbial community in the E-waste dismantling area.  
837 *J Hazard Mater.* **444**, 130379.

838 Yan, K., Zhou, J., Feng, C., Wang, S., Haegeman, B., Zhang, W., Chen, J., Zhao, S.,  
839 Zhou, J., Xu, J., Wang, H., 2023b. Abundant fungi dominate the complexity of  
840 microbial networks in soil of contaminated site: High-precision community  
841 analysis by full-length sequencing. *Sci Total Environ.* **861**, 160563.

842 Yang, L., Lu, H., Yu, X., Li, H., 2022. Carbon dioxide flux in the drained drawdown  
843 areas of Three Gorges Reservoir. *Front Environ Sci.* **10**, 1015888.

844 Yang, P., Yang, H., Sardans, J., Tong, C., Zhao, G., Peñuelas, J., Li, L., Zhang, Y., Tan,  
845 L., Chun, K.P., Lai, D.Y.F., 2020. Large spatial variations in diffusive CH<sub>4</sub> fluxes  
846 from a subtropical coastal reservoir affected by sewage discharge in Southeast  
847 China. *Environ Sci Technol.* **54**, 22, 14192–14203.

848 Ye, C., Li, S., Zhang, Y., Zhang, Q., 2011. Assessing soil heavy metal pollution in the  
849 water-level-fluctuation zone of the Three Gorges Reservoir, China. *J Hazard  
850 Mater.* **191**, 366-372.

851 You, Q., Yan, K., Yuan, Z., Feng, D., Wang, H., Wu, L., Xu, J., 2024. Polycyclic  
852 aromatic hydrocarbons (PAHs) pollution and risk assessment of soils at  
853 contaminated sites in China over the past two decades. *J Clean Prod.* **450**, 141876.

854 Yuan, S., Han, X., Yin, X., Su, P., Zhang, Y., Liu, Y., Zhang, J., Zhang, D., 2023.  
855 Nitrogen transformation promotes the anaerobic degradation of PAHs in water  
856 level fluctuation zone of the Three Gorges Reservoir in Yangtze River, China:  
857 Evidences derived from in-situ experiment. *Sci Total Environ.* **864**, 161034.

858 Zhang, K., Chen, X., Xiong, X., Ruan, Y., Zhou, H., Wu, C., Lam, P.K.S., 2019. The  
859 hydro-fluctuation belt of the Three Gorges Reservoir: Source or sink of  
860 microplastics in the water? *Environ Pollut.* **248**, 279-85.

861 Zhang, S., Li, X., He, D., Zhang, D., Zhao, Z., Si, H., Wang, F., 2022. Per- and poly-  
862 fluoroalkyl substances in sediments from the water-level-fluctuation zone of the  
863 Three Gorges Reservoir, China: Contamination characteristics, source  
864 apportionment, and mass inventory and loadings. *Environ Pollut.* **299**, 118895.

865 Zhang, W., Sun, H., Liang, Y., Tang, X., Fang, Y., Cui, J., Wang, X., Zhou, Q., 2021.  
866 Reservoir operation-induced hydrodynamic disturbances affect the distributions of  
867 Cd, Cu, and Pb in the riparian soil of the water-level-fluctuation zone. *J Soils  
868 Sediments.* **21**, 2343-56.

869 Zhang, Y., Lyu, M., Yang, P., Lai, D.Y.F., Tong, C., Zhao, G., Li, L., Zhang, Y., Yang,  
870 H., 2021. Spatial variations in CO<sub>2</sub> fluxes in a subtropical coastal reservoir of  
871 Southeast China were related to urbanization and land-use types. *J Environ Sci.*  
872 **109**, 206-218.

873 Zhou, Y., Ding, D., Zhao, Y., Li, Q., Jiang, D., Lv, Z., Wei, J., Zhang, S., Deng, S.,  
874 2024. Determining priority control toxic metal for different protection targets  
875 based on source-oriented ecological and human health risk assessment around gold  
876 smelting area. *J Hazard Mater.* **468**, 133782.